日本医放会誌：47（4），565—574，1987（昭62）

Experimental Studies on the Detection of Enlarged Lymph Nodes and Defects Through the Use of Multi-directional Radiography, Macroradiography and CT Lymphography

Teiichi Nakajima, Toshiyuki Okumura, Hideo Tatsuzaki and Masayoshi Akisada
Department of Radiology, Institute of Clinical Medicine, University of Tsukuba

Research Code No.: 510.1, 9

Key Words: Lymph node phantom, Multi-directional radiography, CT Lymphography

ファントームを用いた造影リンパ節同定のための実験的研究

筑波大学臨床医学系（放射線医学）
中島　禎一　　奥村　敏之　　立崎　英夫　　秋貞　雅祥

（昭和61月6月23日受付）
（昭和61年9月8日最終原稿受付）

リンパ造影の診断を正確に行う手段として多方向撮影，拡大撮影およびCTがある．その診断能を，ヨウ素を含んだ造影リンパ節モデルと，血管モデルを組み込んだファントームを用いて解析し，臨床例で，リンパ造影の読影に役立たせようとした．

正常，良性病変，転移リンパ節の計8種類の造影リンパ節モデルを作製し，ファントーム内に備え付け多方向撮影を行った．projection difference indexによる定量的評価は，転移リンパ節と他との鑑別に有効であった．5mm程度の欠損像は，多方向撮影のどの撮影方向においても，十分検出できたが，拡大撮影によってさらに詳細な観察が可能である．

また同じファントームのCT検査を施行し，リンパ造影後のCT検査の評価を行った．最適なウインドウ幅，ウインドウレベルを選ぶことで，リンパ節同志の重なり合いと，リンパ節の欠損との鑑別や，リンパ節内の小欠損の検出が，十分可能であった．

I) Multi-directional Radiography and Macroradiography of Lymph Nodes

I. Introduction

In lymphangiography, the following radiographic methods are employed as means for enabling detailed and accurate diagnoses: 1) multi-directional plain radiography; 2) macroradiography[1]; 3) stereoradiography; 4) conventional tomography; and 5) computed tomography (CT). Multi-directional plain radiography is the most conventional method; radiograms are usually taken from four directions to obtain the followings: An A-P view, a lateral view, and both 45° oblique views. In this method, it is possible to eliminate overlapping areas between lymph nodes and bone or other lymph nodes, and obtain complete information concerning the shape, internal structure, and thickness of the lymph nodes.

M. Wiljasalo[2] introduced the concept of a projection difference index (PDI) in an attempt to differentiate between benign and malignant lymph nodes. In the present study, normal and abnormal lymph node models were superimposed upon blood vessel models to verify the diagnostic capability of Wiljasalo's concept.

II. Procedure

1. Phantom

The lymph node models are composed of polyester resin (Z_{eff} 6.45) mixed with iodine. That is, 20g of iodine crystals are dissolved into 80g of 96% ethyl alcohol, producing a 20% iodine solution. Ten g of this solution is then mixed with 90g of polyester resin, and the resulting 2% iodine-polyester resin mixture is poured into molds, forming 8 types of lymph node models (No. 1—No. 8) (Fig. 1). No. 2 and Nos. 5—8 are the spherical type, resembling thickened, metastatic lymph nodes and have a circular shape from both frontal and lateral views. No. 5—8 have a 3—11.5mm defect in the 19mm-diameter sphere. Nos. 1 and 4 are the saucer type, resembling normal lymph nodes, and having a circular shape from the frontal view and a flat shape from the lateral view. No. 3 is the elliptic type, modelled after slightly swollen lymph nodes seen

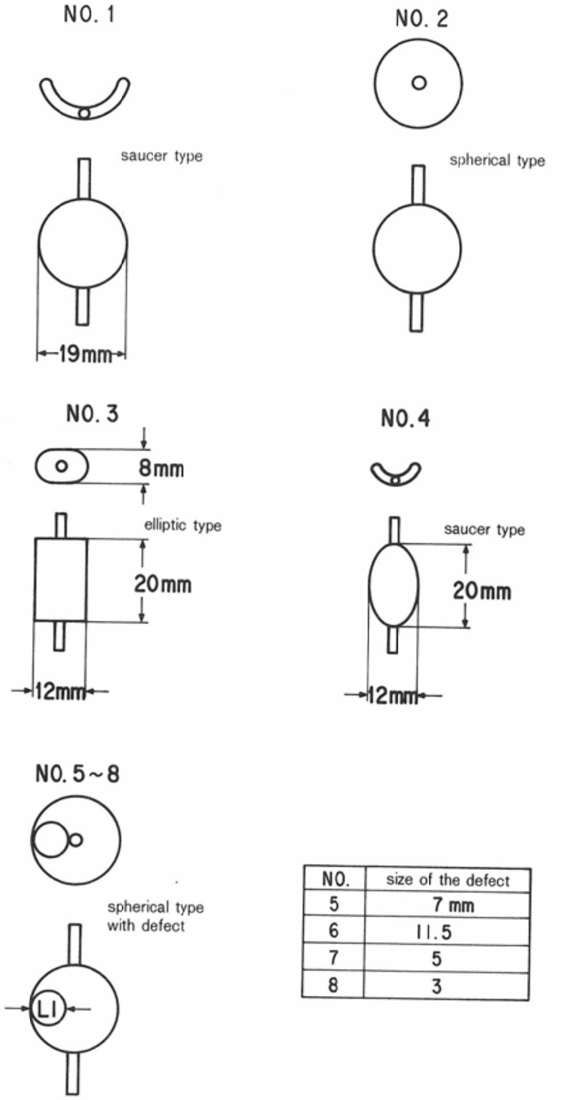

NO.	size of the defect
5	7 mm
6	11.5
7	5
8	3

Fig. 1 Models of normal, swollen, and metastatic lymph nodes, top and en face view. No. 1: saucer type (normal lymph node); No. 2: spherical type (swollen lymph node) No. 3: elliptic type (slightly swollen lymph node); No. 4: saucer type (normal lymph node); Nos. 5—8: spherical type with defect (metastatic lymph node).

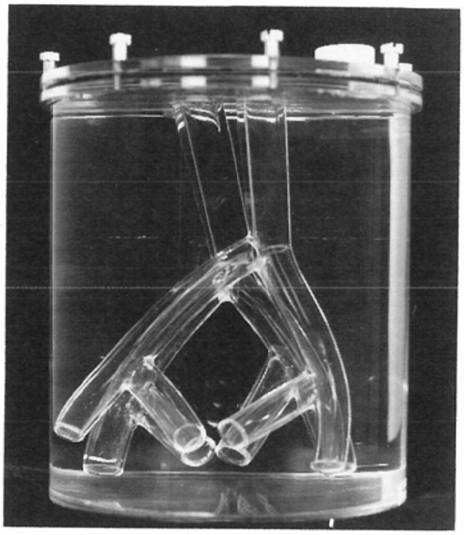

Fig. 2 Blood vessel model within the container.

frequently in lymphogram of urogenital malignancy patients, and having an elliptic shape from both frontal and lateral views.

Blood vessel models (same outer diameter=18mm, varying wall thickness=from 1.5—4mm) of the aorta, inferior vena cava, and iliac artery and vein were placed in an acrylic resin container (Z_{eff}: 6.4, diameter=18.8cm, height=21.5cm, thickness=5mm) (Fig. 2).

The aorta and iliac arteries were filled with 0.76% and the inferior vena cava and iliac veins were filled with 0.57% of Urografin®. The container was filled with distilled water.

2. Radiographic conditions and method of analysis

The X-ray apparatus employed was a Toshiba KXO 1250 (focus=1.0mm, FFD=105cm), the intensifying screen was a Toshiba EM, and the film was Fuji RX. Radiography was performed under the following conditions: 60kVP, 200mA, 0.3 seconds, Bucky (+).

After the lymph nodes models were attached to the blood vessel models within the phantom, radiography was performed under the above-mentioned conditions from 3 different directions to obtain an A-P view and both oblique views (RAO and LAO views) (Fig. 3a, b, c).

Spherical type lymph node models (No. 2), modelled after swollen superficial inguinal lymph nodes, were placed on the outside of the container and were compared with metastatic lymph node models of the same size and shape (Nos. 7 and 8) attached to the blood vessels (Fig. 4).

In order to evaluate and compare differences in thickness from radiography taken from different angles in a quantitative manner, a Projection Difference Index (Wiljasalo) (PDI, Px%) was determined. Px% can be obtained with the following equation:

$$Px\% = \frac{(a-b)}{b} \times 100\%$$

a: maximum width of lymph node

b: minimum width of lymph node

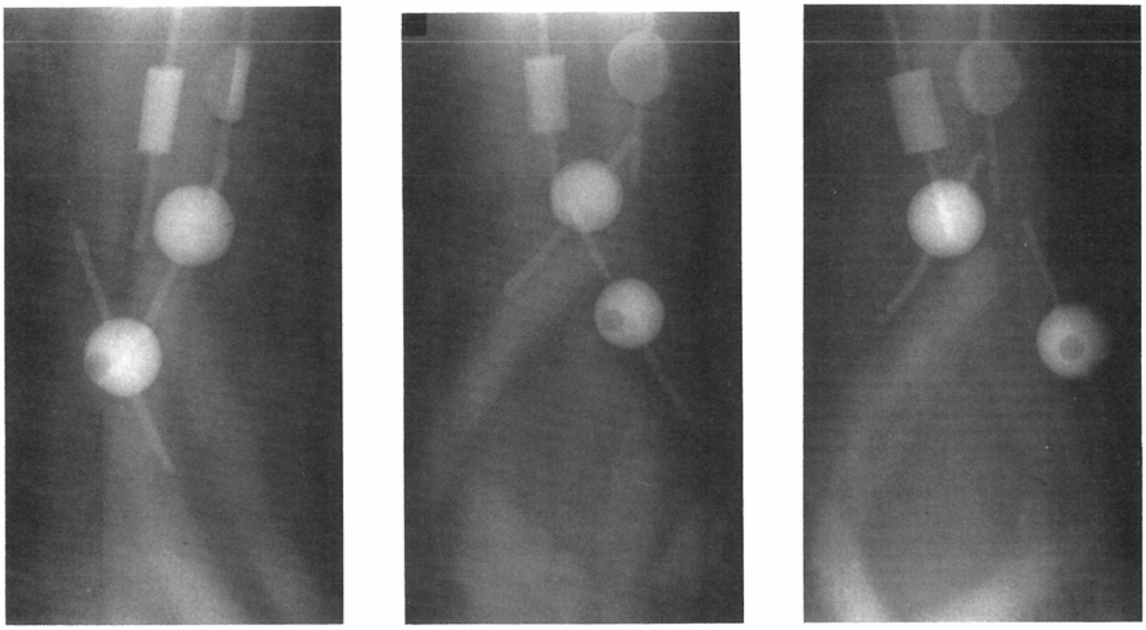

a. RAO view b. AP view c. LAO view

Fig. 3 No. 1, 3, 2, 5 lymphnode model was attached to the blood vessel model respectively for a comparison of PDI values between normal and swollen lymphnodes within the pelvic space.

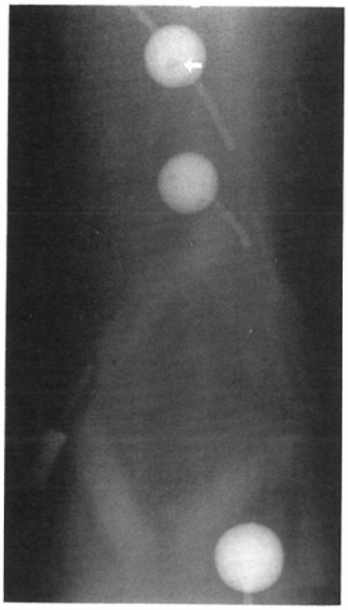

Fig. 4 Spherical type lymphnode model (No. 2) was placed on the outside of the container which appeared to be 1.3 times greater in area compared with same size and shape of lymphnode model (No. 7 and 8) attached to the blood vessel model. The 5mm defect could be seen clearly (arrow).

Table 1 The value of PDI (Px %)

lymph node No.		multi-directional radiography			Px %
		RAO	AP	LAO	
Fig. 3	No. 1	13mm	19mm	19mm	46.2%
	No. 2	22	23	23	4.5%
	No. 3	10	14	14	40.0%
	No. 5	22	23	23	4.5%
Fig. 4	No. 2	—	—	26	—
	No. 3	10	12	15	50.0%
	No. 4	15	15	8	87.5%
	No. 8	23	22	22	4.5%

III. Results

The values of the PDI (Px%) obtained from the radiograms taken from 3 different directions are shown in Table 1. The PDI was 40—87.5% for the saucer and elliptic type, whereas they were 4.5% for the spherical type (swollen nodes) respectively.

The lymph node model (No. 2), attached to the outer surface of the container in order to simulate a swollen superficial inguinal node, appeared to be 1.3 times greater in area compared with a lymph node model of the same size and shape attached to the aorta.

The 5mm defect could be seen clearly ; but the 3mm defect could not be identified easily. However, when macroradiography was performed, it became possible to identify the 3mm defect clearly (Fig. 5).

IV. Discussion

Although the paraaortic lymph nodes and the internal iliac lymph nodes have a tendency to be small and spherical, normal lymph nodes of the "lymphatic skeleton" are generally flat and elliptical, and are linked to the pulsating arterial wall. On the other hand, metastatic lymph nodes are usually thickened and spherical in shape.

As shown in Table 1, the PDI decreases as the normal flat nodes progressively thicken due to cancer metastatis ; for spherical type nodes, the value is only 4.5%. Because the object-film distance varies slightly when the direction of radiography is changed, the PDI will never be 0%, even for spherical lymph nodes. In clinical applications, the PDI is an effective means for differentiating metastatic lymph nodes from normal or benign ones.

PDI of clinical cases were obtained by M. Wiljasalo. His results showed that 97.2% of 373 normal nodes and 72 benign ones had a Px%$\geqq$20, and 91.9% of 62 metastatic nodes had a Px%<20.

When observing, lymphographically, the change in the size of a lymph node over time, it is necessary to

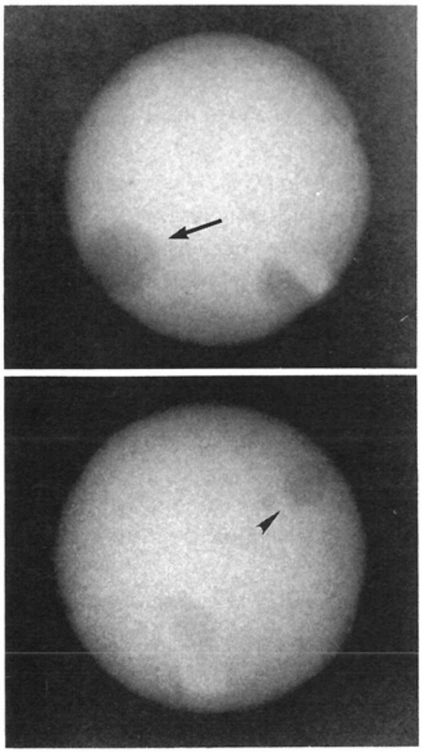

Fig. 5 By 2.5 times macroradiography, 5mm defect (arrow) (No. 7) and 3mm defect (arrow head) (No. 8) could be seen clearly, respectively.

take radiograms under constant conditions in order to determine the effectiveness of the treatment.

Concerning limitations on size when detecting defects, m. Wiljasalo states that detection is possible for defects over 5mm. In Fig. 4, lymph node models of a 5mm defect (No. 7) and a 3mm defect (No. 8) are attached to the aorta. When this figure is compared with the image in Fig. 3 of a lymph node model of a 7mm defect (No. 5) at the position of the iliac artery, both the 5mm and 3mm defects can be detected to a certain extent, but not as obviously as the 7mm defect. Although other complex factors such as patient movement, respiratory movement, and arterial pulsation need to be considered, the present phantom experiment had success in detecting defects over 5mm. On the contrary, it is difficult to differentiate these tiny metastatic defects from those due to hyperplastic follicles. Thus, in order to discriminate between the two, it is necessary to study the internal structure of lymph nodes in more detail. Macriradiography is an attempt to accomplish this task[3]. Macroradiograms of Nos. 7 and 8 are shown in Fig. 5 ; even a 3mm defect can easily be detected. The diagnostic value of macroradiography was further studied in clinical use[4].

V. Conclusion

Through phantom experiments employing lymph node and blood vessel models, X-ray analysis of lymphography was conducted based on the concepts of length, width, and thickness originally proposed by M. Wiljaslo. It was found that the above concept was an effective means for differentiating metastatic lymph nodes from normal ones. Although it was possible to detect 5mm defects from multi-directional plain radiography, macroradiography made more detailed observation possible, that is, even 3mm defects could be observed through the phantom experiment.

II) CT Lymphography

I. Introduction

When both lymphography and CT are employed in the determination of the stages of a malignant tumor, CT can be performed either prior to lymphography (prelymphographic CT with/without contrast enhancement (CE)), or subsequently (post lymphographic CT). In the latter method, it is possible to observe several artifacts arising from high CT values of contrast material[5)6)].

In this study, as part of basic research into the diagnostic capabilities of postlymphographic CT, phantom experiments were conducted in order to study artifacts, defect detection capability, discrimination of lymph node overlapping, and optimal conditions for CT image.

II. Material and Methods

Based on data obtained from lymphograms of clinical cases, a diluted solution of 76% Urografin® was poured into the aorta and the iliac arteries to a CT value of 120 H.U., and into the inferior vena cava and iliac veins to a CT value of 100 H.U., in accordance with the conditions under which CE with venous injection was conducted.

The CT values of the lymph node models (Nos. 1—8) (Fig. 1) were between 600 and 800 H.U., roughly equivalent to the CT values of an opacified lymph node of the patient approximately one week after lymphography.

The CT apparatus employed was a GE CT/T 8800, scan conditions were 120kVP, 200mA, and scanning time was 5.8 seconds. A Yokokawa multi-format camera was used, with Kodak NMB film.

The lymph node models were attached to the container as shown in Fig. 6 and 7, scanning was conducted twice, once for a 5mm-thick slice, and again for a 10mm-thick slice.

Radiographic conditions were set at conditions under which blood vessels and lymph nodes are revealed clearly (window width, 500—600, window level, 100—150). Furthermore, for measurement of defects, the value of the level was assigned to be the average of the CT values of the defect and the opacified lymph node. All phantom experiments were conducted under static conditions.

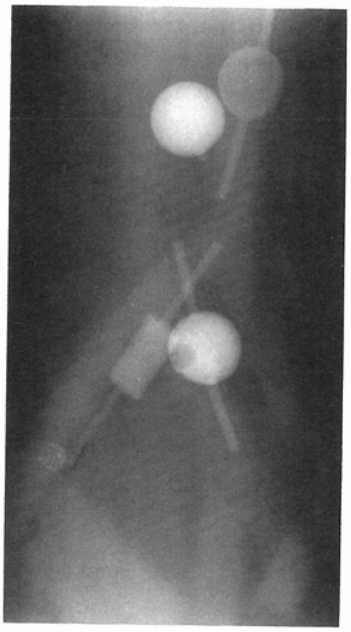

Fig. 6 No. 1, 2, 5, 3 lymphnode model attached to the blood vessel model, respectively.

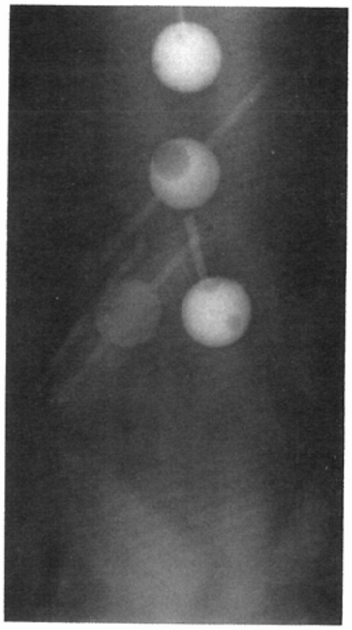

Fig. 7 No. 8, 6, 7, 1 lymphnode model attached to the blood vessel model, respectively.

III. Results

1) Window width

Overlapping or conglomerate formations of lymph nodes could be distinguished by raising the window width.

a, window width 500 (Fig. 8a)

b, window width 1,000 (Fig. 8b)

In b, it was possible to discriminate 2 different lymph nodes.

2) Slice thickness

Scanning was performed at a constant window level for the two thicknesses below :

a, 5mm-thick slice

b, 10mm-thick slice

The partial volume effect was more prominent in the 10mm-thick slice (Fig. 9a) than the 5mm-thick slice (Fig. 9b).

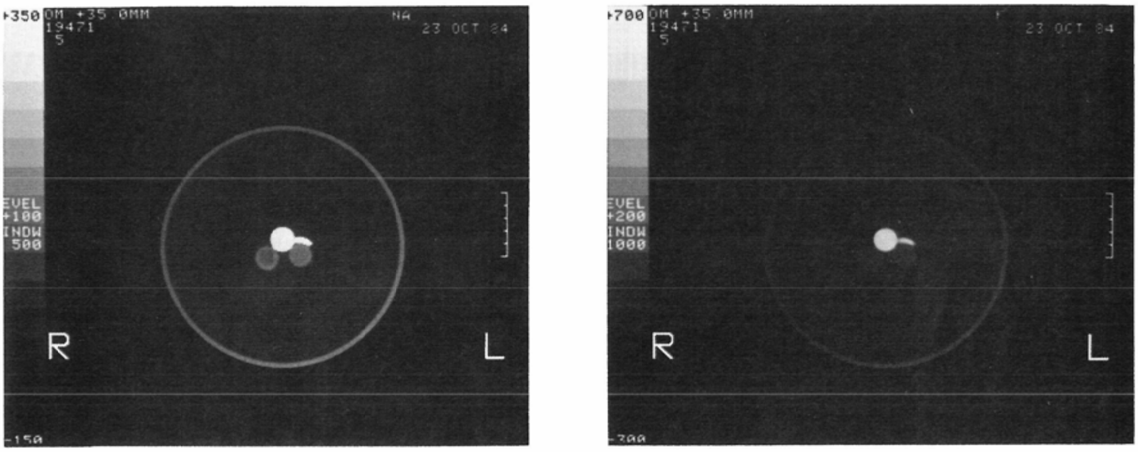

8a 8b

Fig. 8 Comparison of each CT image at the same level.

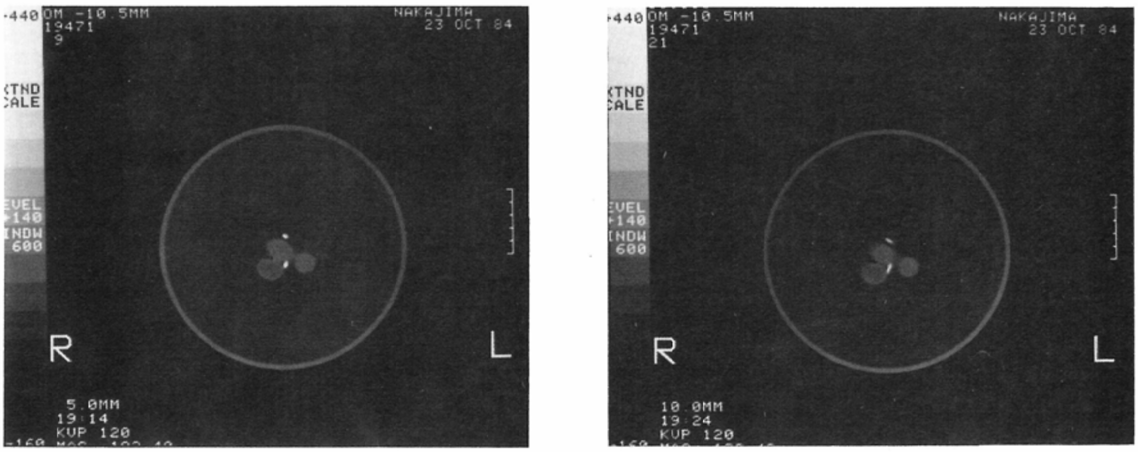

9a 9b

Fig. 9 Scanning was conducted twice at the same level, once for a 5mm-thick slice (a), again for a 10mm-thick slice (b).

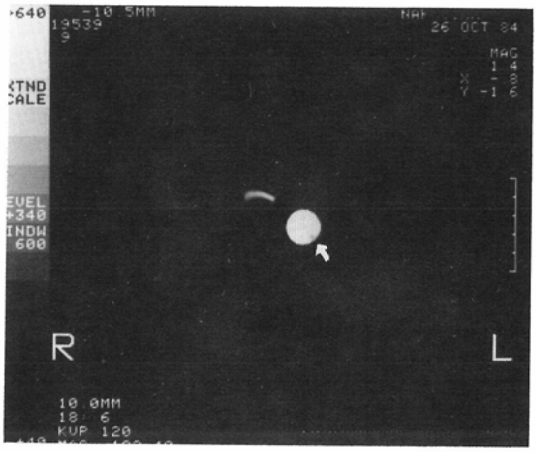

Fig. 10 3mm defect (arrow) could be detected under optimal conditions.

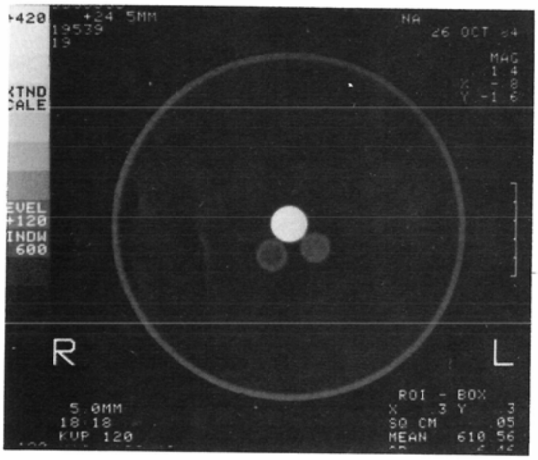

11a

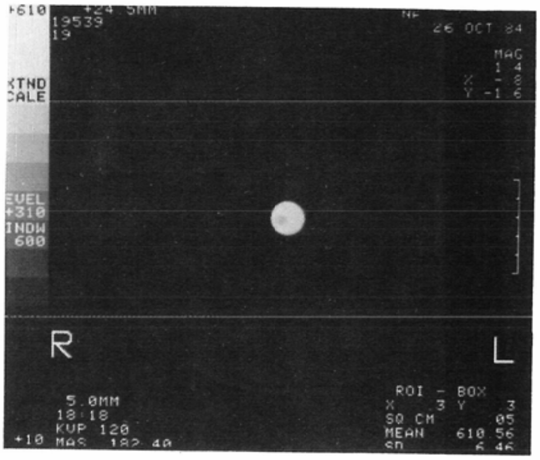

11b

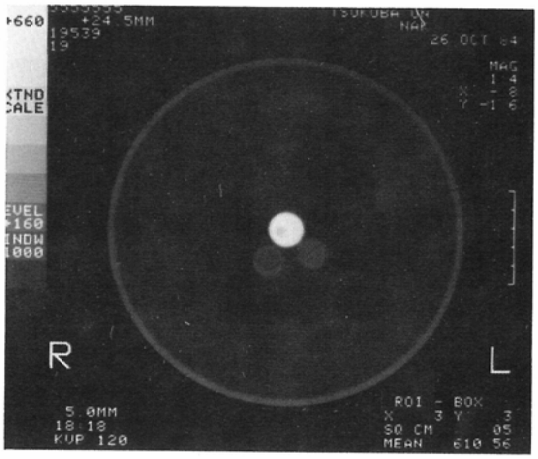

11c

Fig. 11(a,b,c) The defect of the lymphnode model could be seen differently under the various CT conditions.

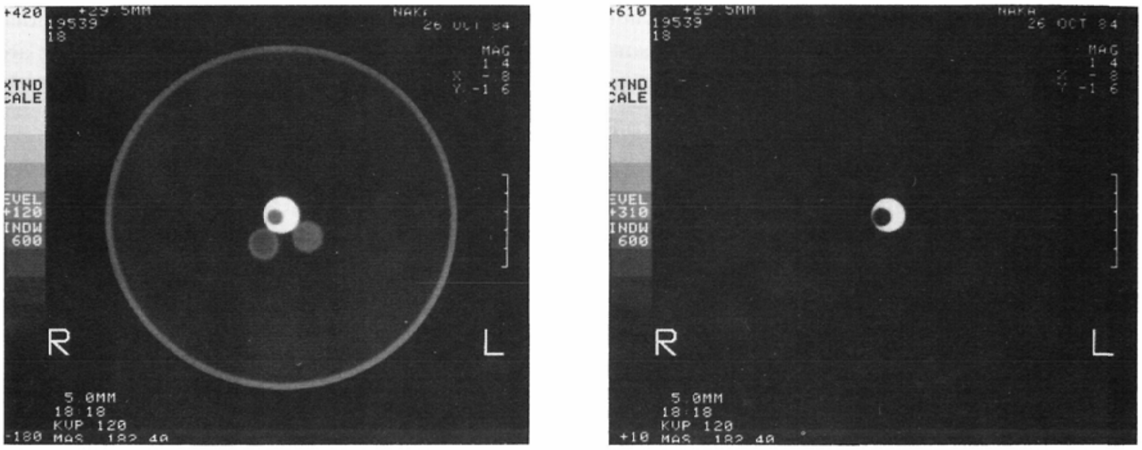

12a 12b

Fig. 12 CT image at the same level. The size of the defect was measured most accurately under the condition of (b).

Under optimal conditions (window width 600, window level 340), it was possible to detect even 3mm defects (No. 8 in Fig. 1) (Fig. 10).

Under CT conditions (window width 600 and window level 120) (No. 6 in Fig. 1), even a 6.6mm defect was sometimes undetected, Fig. 11a ; whereas scanning with a window sidth and level of (b) and (c) revealed the defects.

b), window width 600, window level 310.

c), window width 1000, window level 160.

In order to identify defects under same CT conditions as in Fig. 11a, it was necessary for the defect to be over 1cm in size (Fig. 12a).

IV. Discussion

Although artifacts resulting from highly opacified lymph nodes are mentioned as a drawback of post-lymphographic CT examination, obvious artifacts were not produced in these phantom experiments. Consequently, efforts to minimize body movement during scanning make it possible to obtain a clear image in clinical cases as well. During CT examination, peristalsis and respiratory movement are suppressed by the administration of parasympathetic blockers and holding the breath, respectively. The problem is the pulsating movement of the arteries, to which the lymph nodes are closely attached.

Seibert[7] conducted a phantom experiment concerning measurement of the size of spinal cord by metrizamide CT. According to Seibert, when the window was set equal to the averaged CT value of the spinal cord and opacified thecal sac, the measured size of the spinal cord most nearly approximated its actual size. Applying his findings to this study, the size of the defect was measured by assigning the average CT value of the defect and the lymph node to the value of the window level which was verified in this experiment (Fig. 12b).

Under optimal conditions, this CT method has a detection capability of 3mm defects nearly equivalent to that of macroradiography. However, at clinical CT conditions (window width ca. 400 and level ca. 120), small defects could not be observed due to the partial volume effect. Since 10mm-thick slices are common in actual clinical situations, a size of over 10mm is necessary for the reliable detection of defects. In conventional lymphography, 10mm is the size for which detection of defects can be made with certainty[8] ; and, as mentioned earlier, it is also possible to detect 3mm defects by macrolymphography.

V. Conclusion

Post-lymphographic CT analysis was conducted. By reducing the slice thickness, it was possible to obtain a better image with less partial volume effect. By making the slices thinner, or by selecting an optimal window width and level, it was possible to discriminate overlapping of lymph nodes or to detect defects within the lymph nodes. However, in routine CT examination, it is not possible to detect defects unless they are over 1cm in diameter.

References

1) Lüning, M.: Zusatzuntersuchungen zum Lymphogramm. Lymphographie bei malignen Tumoren edited by Lüning, M., Wiljaslo, M. and Weissleder. H., Georg Thieme, Stuttgard p. 254, 1983
2) Wiljasalo, M.: Lymphographic differential diagnosis of neoplastic diseases. Acta Radiol. (Stokh) Suppl 247, pp. 33—42, 1965
3) Nakajima, T. and Akisada, M.: Significant application of macroradiography to lymphography. (in Japanese) Japan J. Lymphology, 6: 73—75, 1983
4) Nakajima, T.: Basic and clinical study of lymphography. Ph.D. Thesis, University of Tsukuba, 1984.
5) Ginaldi, S., Wallace, S., Jing, B.-S. and Bernardino, M.E.: Carcinoma of the cevrix. Lymphography and CT. Amer. J. Roentgenol., 136: 1087—1091, 1981.
6) Castellino, R.A., Hoppe, R.T., Blank, N., Young, S.W., Neumann, C., Rosenberg, S.A. and Kaplan, H.S.: CT, lymphography and staging laparotomy. Correlations in initial staging of Hodgkin's disease. Amer. J. Roentgenol., 143: 37—41, 1984
7) Seibert, C.E., EdBarnes, J., Dreisbach, J.N., Swanson, W.B. and Heck, R.J.: Accurate CT mesurement of the spinal cord using metrizamide: Physical factors. Amer. J. Roentgenol., 136: 777—780, 1981.
8) Peters, P.E.: Lymphography: Overview. Radiology today I. edited by M.W. Donner and F.H.W. Heuck. Springer-Verlag, Berlin-Heidelberg, pp. 315—326, 1981.